PROCEEDINGS OF SCIENCE

Measurements of the muon content of EAS in KASCADE-Grande compared with SIBYLL 2.3 predictions

J.C. Arteaga-Velázquez*[1], D. Rivera-Rangel[1], W.D. Apel[2], K. Bekk[2], M. Bertaina[3], J. Blümer[2,4], H. Bozdog[2], I.M. Brancus[5], E. Cantoni[3,6], A. Chiavassa[3], F. Cossavella[4], K. Daumiller[2], V. de Souza[7], F. Di Pierro[3], P. Doll[2], R. Engel[2], D. Fuhrmann[8], A. Gherghel-Lascu[5], H.J. Gils[2], R. Glasstetter[8], C. Grupen[9], A. Haungs[2], D. Heck[2], J.R. Hörandel[10], D. Huber[4], T. Huege[2], K.-H. Kampert[8], D. Kang[4], H.O. Klages[2], K. Link[4], P. Łuczak[11], H.J. Mathes[2], H.J. Mayer[2], J. Milke[2], B. Mitrica[5], C. Morello[6], J. Oehlschläger[2], S. Ostapchenko[12], N. Palmieri[4], T. Pierog[2], H. Rebel[2], M. Roth[2], H. Schieler[2], S. Schoo[2], F.G. Schröder[2], O. Sima[13], G. Toma[5], G.C. Trinchero[6], H. Ulrich[2], A. Weindl[2], J. Wochele[2], J. Zabierowski[11] - KASCADE-Grande Collaboration

[1] *Universidad Michoacana, Inst. Física y Matemáticas, Morelia, Mexico*
[2] *Institut für Kernphysik, KIT - Karlsruhe Institute of Technology, Germany*
[3] *Dipartimento di Fisica, Università degli Studi di Torino, Italy*
[4] *Institut für Experimentelle Kernphysik, KIT - Karlsruhe Institute of Technology, Germany*
[5] *Horia Hulubei National Institute of Physics and Nuclear Engineering, Bucharest, Romania*
[6] *Osservatorio Astrofisico di Torino, INAF Torino, Italy*
[7] *Universidade São Paulo, Instituto de Física de São Carlos, Brasil*
[8] *Fachbereich Physik, Universität Wuppertal, Germany*
[9] *Department of Physics, Siegen University, Germany*
[10] *Dept. of Astrophysics, Radboud University Nijmegen, The Netherlands*
[11] *National Centre for Nuclear Research, Department of Astrophysics, Lodz, Poland*
[12] *Frankfurt Institute for Advanced Studies (FIAS), Frankfurt am Main, Germany*
[13] *Department of Physics, University of Bucharest, Bucharest, Romania*
E-mail: arteaga@ifm.umich.mx

The KASCADE-Grande observatory was a ground-based air shower array devoted to the study of the energy and composition of cosmic rays with energies from 1 PeV to 1 EeV. The experiment consisted of different detector systems which allowed the simultaneous measurement of distinct components of the air showers (EAS), such as the muon content. In this contribution, we study the total muon number and the lateral density distribution of muons in EAS detected by KASCADE-Grande. The data are analyzed as a function of the zenith angle and the total number of charged particles. The attenuation length of the muon content of EAS is also measured. The results are compared with the predictions of the SIBYLL 2.3 hadronic interaction model.

35th International Cosmic Ray Conference — ICRC2017
10–20 July, 2017
Bexco, Busan, Korea

*Speaker.

1. Introduction

Hadronic interaction models are a key element in the analysis of data from extensive air showers (EAS) induced by cosmic rays in the atmosphere. However, they are subject to important uncertainties, which may hamper cosmic-ray analysis. Recently, a lot of progress has been done towards the reduction of such uncertainties, in part, thanks to the data provided by the LHC [1]. In this regard, one of the models that has been updated is SIBYLL [2].

In this work, we will test the muon predictions of the post-LHC model SIBYLL 2.3 using the data of the KASCADE-Grande observatory [3]. For these tests, we study shower muons since they are direct messengers of the hadronic processes occurring early in the shower [4]. Hence a failure of the model to describe the observed muon data of EAS may imply a problem in the description of the hadronic physics of the EAS.

2. The KASCADE-Grande observatory

KASCADE-Grande was a ground-based air-shower observatory dedicated to investigate the energy spectrum, the elemental composition and the arrival direction of cosmic rays in the energy range from 10^{15} and 10^{18} eV [3]. The instrument was located at the Karlsruhe Institute of Technology, Campus North (110 m a.s.l.) in Karlsruhe, Germany and consisted of several detector systems aimed to measure with high precision different components and properties of the EAS. For example, the shower size or total number of charged particles (electrons plus muons) ($E_{th} > 3\,\mathrm{MeV}$), the shower core position and the angle of incidence were estimated from data collected with the $0.5\,\mathrm{km}^2$ main array, called Grande, composed by 37 scintillator detectors separated by a mean distance of 137 m. Meanwhile the total number of muons ($E_{th} > 230\,\mathrm{MeV}$) was obtained from local muon density measurements performed with the 192 shielded detectors of the $200 \times 200\,\mathrm{m}^2$ KASCADE array [3]. Systematic uncertainties for N_{ch} and N_{μ} were calculated as described in [3] and [5], respectively. They were found to be $\leq 15\%$ and $\leq 25\%$, correspondingly.

3. MC simulations and experimental data

For the tests aimed at this work MC data sets were built using SIBYLL 2.3 [2] and Fluka 2011.2 [6] as high- and low-energy ($E_h \leq 200\,\mathrm{GeV}$) hadronic interaction models, respectively. The production and development of the shower were simulated with CORSIKA 7.5 [7], while the response of the detector to the passage of the shower, with a GEANT 3.21 [8] based program. MC events were generated for zenith angles $\theta < 42^\circ$ and the energy interval between $E = 10^{14}\,\mathrm{eV}$ and $3 \times 10^{18}\,\mathrm{eV}$ using an E^{γ} primary spectrum with spectral index $\gamma = -2$. For the analysis, the MC events were weighted in order to simulate an E^{-3} power-law spectrum, which is in better agreement with the experimental data (see, for example, [5]). MC data samples were produced for five primary nuclei: H, He, C, Si and Fe. An extra data set, called mixed, where the above nuclei are present in equal abundances, was also created from the aforementioned data sets. In total, $\sim 1.2 \times 10^7$ MC showers were generated. All of them were processed with the same algorithm employed with the experimental data [3].

With regard to the measured data, we have considered events collected during the full data acquisition period of the experiment, i.e., from December 2003 up to November 2012. Here, several selection cuts were applied in order to reduce the effect of systematic uncertainties in the muon data. In particular, we only considered events that were measured during stable data acquisition

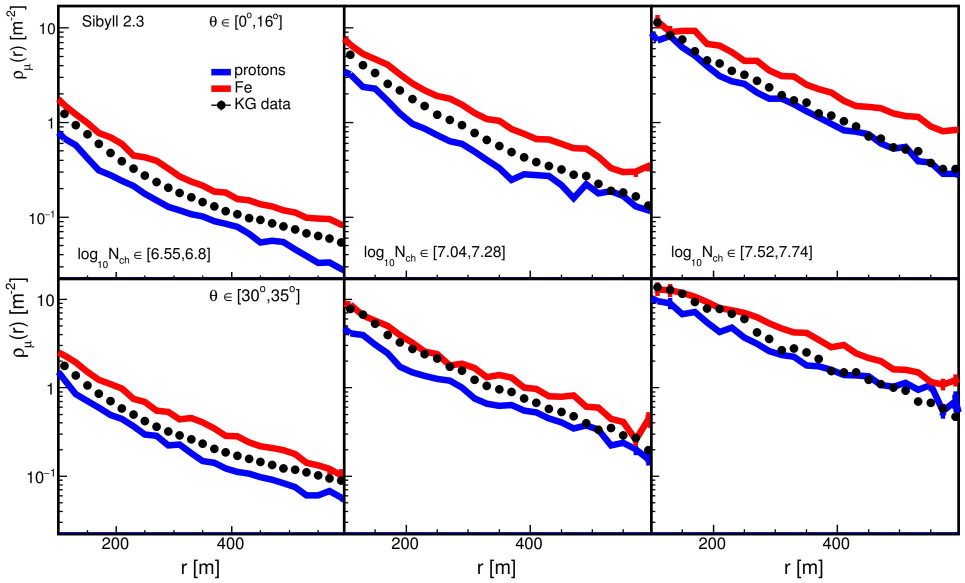

Figure 1: Mean muon lateral distribution functions of EAS measured with KASCADE-Grande (points) compared with the predictions of SIBYLL 2.3 for iron (red upper lines) and proton (lower blue lines) primaries. Statistical error bars in measured data are smaller than the size of the markers

runs with no hardware problems. In addition, we included events that have passed successfully the full reconstruction chain [3]. Besides, the EAS cores were required to be located within the limits of a central area of $2.2 \times 10^5\,\mathrm{m}^2$ inside the KASCADE-Grande array and within radial distances in the interval $R = [100\,\mathrm{m}, 600\,\mathrm{m}]$ measured from the center of the KASCADE array. On the other hand, we rejected events with $\theta \geq 40°$. Finally, low energy events, which have poorer reconstructed muon numbers, were removed from the data sample by requiring showers that activated more than 11 Grande stations and had a high N_μ number (specifically $\gtrsim 3 \times 10^4$ and $\gtrsim 4 \times 10^4$ for data with $\theta \lesssim 30°$ and $30° \lesssim \theta < 40°$, respectively). These quality cuts were also applied to the MC data sets for the analysis. Using the above selection cuts, we are left with about 1.2×10^7 measured events for the present studies. According to MC simulations the maximum efficiency is reached for $\log_{10}(E/\mathrm{GeV}) = 7.2 \pm 0.3$ and $\log_{10}(N_\mu) = 5.3 \pm 0.3$ depending of the primary particle and the arrival direction. On the other hand, the mean core and angular resolutions were found to be $\leq 11\,\mathrm{m}$ and $\leq 0.7°$, respectively. The bias in the muon size is expected to be smaller than 20% for $\log_{10}(N_\mu) > 5.3$.

4. Checks of SIBYLL 2.3 predictions for shower muons

Muon radial density distributions. The aim of this study is to compare the predictions of SIBYLL 2.3 and the KASCADE-Grande measurements for the mean muon lateral distributions at the shower plane, $\rho_\mu(r)$, at different zenith angles and $\log_{10}(N_{ch})$ intervals. For this purpose, we divide our data in five bins of θ, each of them with equal acceptance: $[0°, 16.71°]$, $[16.71°, 23.99°]$, $[23.99°, 29.86°]$, $[29.86°, 35.09°]$ and $[35.09°, 40°]$. Next, we subdivide these data sets in bins of $\log_{10}(N_{ch})$, in particular, $[6.0, 6.55]$, $[6.55, 6.8]$, $[6.8, 7.04]$, $[7.04, 7.28]$, $[7.28, 7.52]$, $[7,52, 7.74]$ and $[7.74, 8.0]$. Then, for each θ and shower size intervals we build the mean measured $\rho_\mu(r)$ distributions (neglecting atmospheric corrections due to the projection on the shower disk plane),

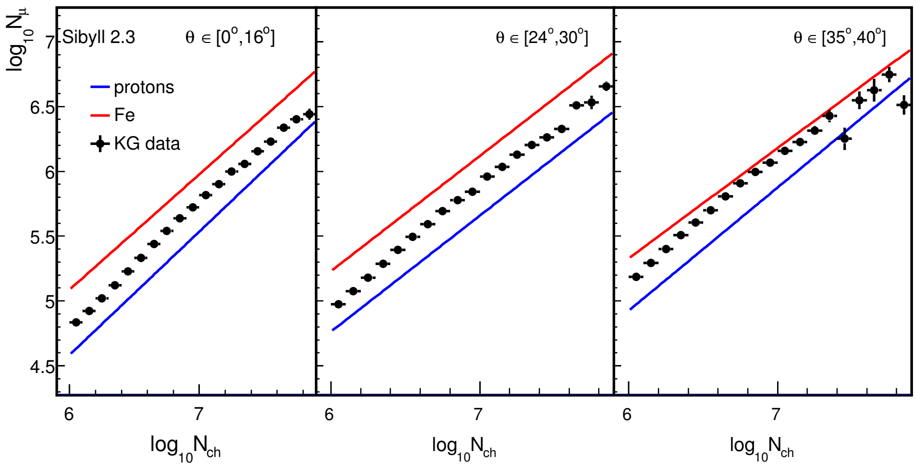

Figure 2: Logarithm of the total muon content versus the logarithm of the total number of charged particles in air showers as measured with the KASCADE-Grande detector (points). Measurements are confronted with predictions of SIBYLL 2.3 for iron nuclei (upper red lines) and protons (lower blue lines). The data covers the energy interval from $E \sim 10^{6.8}$ GeV to $\sim 10^9$ GeV.

which we compare with the respective predictions from SIBYLL 2.3 for pure protons and iron nuclei, respectively. In fig. 1 we show a plot with results for two zenith angle intervals and three distinct shower size ranges. In particular, we observe that the measured distributions are within the MC predictions. In general, that holds for vertical and inclined showers with $\log_{10}(N_{ch}) < 7.74$. For higher values of the total number of charged particles, there are some deviations, but here statistical fluctuations avoid us to drive a conclusion.

The total muon number. In this part of our study, we compare the total muon number (after correction for systematic biases using the correction function defined in [5]) as a function of the shower size as measured with the KASCADE-Grande observatory against the expectations from SIBYL 2.3 for hydrogen and iron nuclei for the aforementioned θ ranges. The results for three distinct zenith angle intervals are presented in fig. 2. In general, we do not observe any deviation of the measured data from the MC simulations. However, we see that for increasing zenith angles the mean composition tends to be heavier, which could be due to a mismatch between the predicted and the measured zenith angle evolutions of the shower muon content of EAS.

The muon attenuation length. In order to study the behaviour of N_μ with θ in air showers, we have determined the attenuation length of muons in the Earth's atmosphere, Λ_μ. This parameter is especially useful for cross-checking hadronic interaction models. Differences between the experimental and expected values of Λ_μ have been previously observed with KASCADE-Grande. For example, in [9] it was reported that the measured Λ_μ deviates from the predictions of the high-energy hadronic interaction models QGSJET-II-2 [10], QGSJET-II-04 [11], EPOS 1.99 [12] and SIBYLL 2.1 [13] in the primary energy interval from $E \sim 10^{16}$ eV to about 10^{17} eV and for EAS with $\theta < 40°$. Statistical and systematic errors (associated to instrumental effects, reconstruction/analysis methods, EAS fluctuations, etc.) can not explain the observed anomaly. The analysis was performed with experimental data registered during the period December 2003 - October 2011. Only events with radial distances, R, between 270 m and 440 m and within an area of $8 \times 10^4\,\mathrm{m}^2$

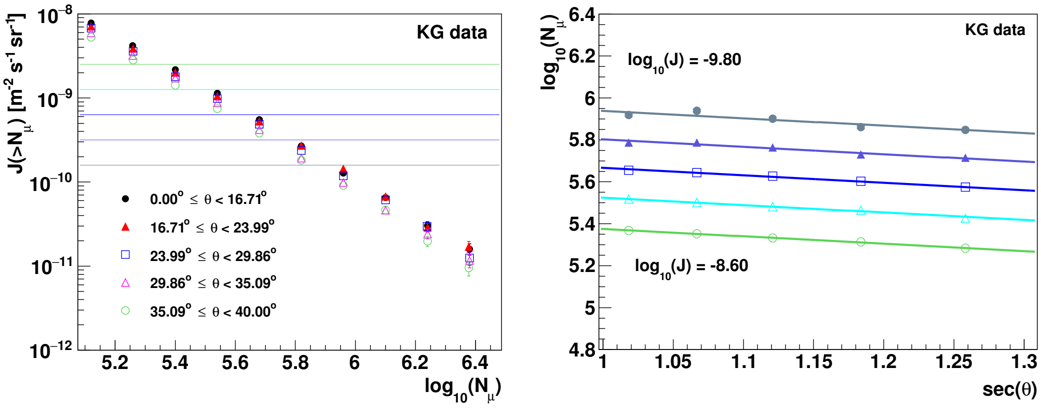

Figure 3: *Left*: Integral muon intensities derived from the measurements with the KASCADE-Grande observatory for five zenith angle intervals [9]. The CIC cuts employed in this work are shown as horizontal lines. *Right*: Muon attenuation curves extracted with the CIC method from the experimental data [9]. The results of the global fit with equation 4.1 are shown with solid lines. The upper curve correspond to the lowest CIC cut.

located at the center of the KASCADE-Grande array were considered, as they further reduce the systematic bias on N_μ. To obtain Λ_μ, the procedure makes use of the constant intensity cut (CIC) method that assumes that the intensity of cosmic rays is isotropic in θ [14]. The method consists of selecting EAS data from different zenith angles by means of cuts applied at fixed frequencies (see 3, left). Actually, data selected along curves with the same integral intensity should correspond to events with the same primary energy but different shower sizes due to the increasing atmospheric depth at high zenith angles. This dependence is expressed in terms of a typical exponential absorption formula, which is parameterized as a function of a single Λ_μ [9] (see fig. 3, right). For our

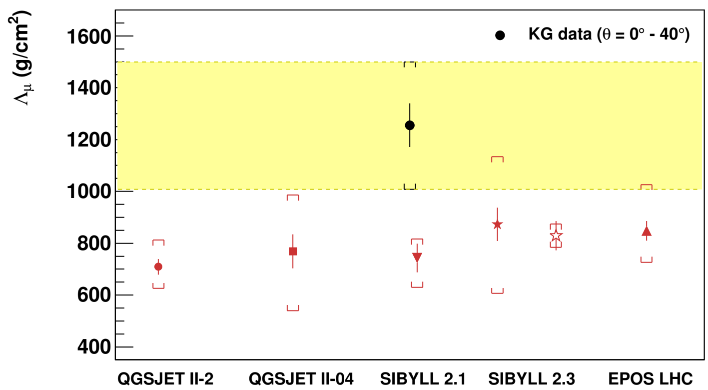

Figure 4: Muon attenuation length measured with the KASCADE-Grande experiment (upper point) compared with predictions of several pre-LHC and post-LHC high-energy hadronic interaction models (lower points) for EAS with core distances within 270 m and 440 m from the KASCADE center and with energies between $E \sim 10^{16}$ eV and $\sim 10^{17}$ eV and using a mixed composition assumption. The total uncertainty (statistical and systematic errors added in quadrature) are shown with squared brackets. Error bars represent statistical uncertainties. The filled and hollowed stars are the predictions from SIBYLL 2.3 for mixed composition and our fitted composition model (see text).

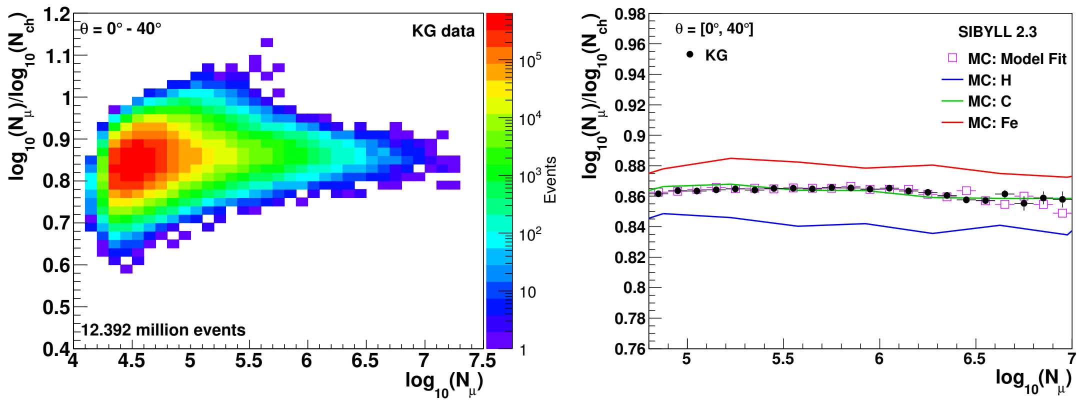

Figure 5: *Left*: The measured distribution for the ratio $Y = \log_{10}(N_\mu)/\log_{10}(N_{ch})$ as a function of the $\log_{10}(N_\mu)$ for selected EAS with $\theta < 40°$. The effective observation time of the data sample is $\Delta t = 1.6 \times 10^8$ s. *Right*: The mean of the experimental Y parameter for the data shown on the left against $\log_{10}(N_\mu)$ (black circles). The respective mean is also shown for predictions of SIBYLL 2.3 for protons (lower blue line), carbon (middel green line), iron nuclei (upper red line) and our fitted composition model (open squares, see text). The MC simulations include the full detector simulation and the EAS reconstruction procedures.

case, we have

$$N_\mu(\theta) = N_\mu^\circ e^{-X_0 \sec(\theta)/\Lambda_\mu}, \tag{4.1}$$

where $X_0 = 1022\,\mathrm{g/cm^2}$ is the vertical column depth at KASCADE-Grande and N_μ°, a normalization factor, which depends on the attenuation curve. The analysis of [9] has been recently updated (details will be published elsewhere). The results are presented in fig. 4. Statistical and total uncertainties are also shown. They were estimated through detailed studies. The experimental systematic error includes the uncertainty due to the calculation procedure, the uncertainty owing to the muon correction function, the systematic error of the corrected muon number and the corresponding composition and model dependence, the uncertainty owing to the size of the θ intervals and the uncertainties associated with the shower core position, R. The MC estimations involve also the uncertainties due to the spectral index of the primary spectrum, γ, and due to the primary composition. The latter is estimated by comparing the value obtained using a mixed composition assumption with the results for the five primary nuclei employed in simulations. We have also carried out a calculation of Λ_μ with the SIBYLL 2.3 data. A preliminary result for the mixed composition assumption is presented in fig. 4. At the moment, its systematic error only includes the uncertainty due to the fit of the attenuation curves and that due to composition, which is the dominant source of uncertainty in our result. We obtain from the aforementioned results that, the measured Λ_μ deviates $1.4\,\sigma$ from the prediction of SIBYLL 2.3. The deviation seems small, but that could be in part due to the large composition error that accompany our prediction.

In order to reduce the systematic uncertainty on the value of Λ_μ predicted by SIBYLL 2.3, we have used a composition model derived from the data itself. The procedure is simple. By using a χ^2 fit, we find the weight parameters for the MC energy spectra of four mass groups (H, He, C, and Si+Fe in a 50 % mixture) that minimize the difference between the measured $Y = \log_{10}(N_\mu)/\log_{10}(N_{ch})$ vs $\log_{10}(N_\mu)$ event distribution (c.f. fig. 5, left) and the predicted one, the latter for the linear combination of the four mass groups. Before weighting, the MC energy

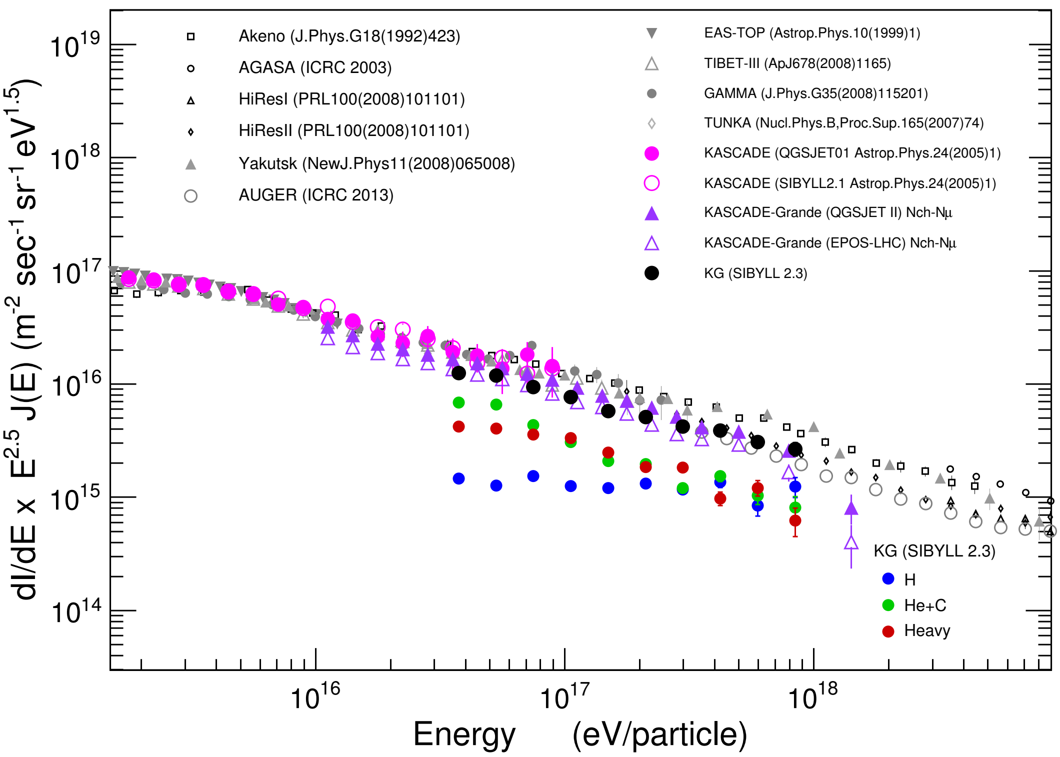

Figure 6: Results of the fit to the measured $Y(N_\mu)$ distributions using SIBYLL 2.3 data and a composition model with four mass groups (H, He, C, and Si+Fe in a 50 % mixture) each of them following a double power-law energy spectrum. The derived all-particle energy spectrum is shown with black dots. The fitted spectra for protons, He+C, and the heavy component of cosmic rays are shown in the lower part of the figure with blue full squares, green open crosses and red open squares, respectively. The aforementioned curves are compared with results of other observatories and previous estimations of KASCADE-Grande for the all-particle energy spectrum.

spectra resemble an E^{-3} power-law function. The fit was performed for $\log_{10}(N_\mu) \geq 4.8$ with the following Chi-square function:

$$\chi^2 = \sum_{i,j} \frac{[n_{ij}^{exp} - \sum_A n_{ijA}^{MC}(\mathbf{p}_A)]^2}{(\sigma_{ij}^{MC})^2}, \tag{4.2}$$

where n_{ij}^{exp} is the number of experimental events for the bin $(Y_i, N_{\mu,j})$ of the respective Y distribution, while n_{ijA}^{MC} is the corresponding number of MC events for the above bin and the mass group A. The widths of the Y and $\log_{10}(N_\mu)$ bins are 0.02 and 0.1, respectively. On the other hand, σ_{ij}^{MC} is the statistical error of n_{ijA}^{MC} and $\mathbf{p}_A$ is a vector with the parameters that define the weights, $\mathbf{w}_A(E)$, of the energy spectrum for A. The weights are applied event-by-event on the MC data according to its true energy, E. They are parameterized using a double power-law formula

$$\mathbf{w}_A(E, \mathbf{p}_A) = p_{0,A} E^{p_{1,A}} \left[1 + \left(\frac{E}{p_{4,A}}\right)^{p_{3,A}}\right]^{(p_{2,A}-p_{1,A})/p_{3,A}}. \tag{4.3}$$

Here the $p_{k,A}$ are free parameters (i.e. the components of $\mathbf{p}_A$). The reason of using these expressions is due to the presence of breaks around $E = 10^{17}$ eV in the energy spectra of the light [15] and the heavy [16] components of cosmic rays. With the results of the fit, we build our composition model using SIBYLL 2.3 data. This is shown in fig. 6. The mean values of $Y(N_\mu)$ for our fitted model and the respective measurements are compared in fig. 5, right. In fig. 6, we observe the heavy knee at $\log_{10}(E/\mathrm{eV}) = 16.80 \pm 0.01$ ($\Delta\gamma = p_2 - p_1 = -0.67 \pm 0.03$). Using this composition model we have calculated Λ_μ. This is presented in fig. 4. The systematic error only includes the uncertainty from the CIC method. It seems that, the predictions from our model for Λ_μ using SIBYLL 2.3 tends to be below the measured data.

5. Conclusions

We have tested muon predictions of SIBYLL 2.3 against measurements of the KASCADE-Grande observatory for $\rho_\mu(r)$ and N_μ at different θ and N_{ch} ranges, as well as for Λ_μ. In general, it seems that $\rho_\mu(r)$ measurements for $\theta < 40^\circ$ and $6.0 \leq \log_{10}(N_{ch}) \leq 7.74$ are within the predictions of the model. For N_μ the agreement is observed up to $\log_{10}(N_{ch}) = 8.0$. On the other hand, we see what appears to be a mismatch between the predicted and measured Λ_μ values when uncertainties due to primary composition are reduced. This reduction was achieved using a nominal composition model based on fits to the $Y(N_\mu)$ distributions of the measured data.

Acknowledgments. The authors would like to thank the members of the engineering and technical staff of the KASCADE-Grande Collaboration, who contributed to the success of the experiment. The KASCADE-Grande experiment was supported in Germany by the BMBF and by the 'Helmholtz Alliance for Astroparticle Physics - HAP' funded by the Initiative and Networking Fund of the Helmholtz Association, by the MIUR and INAF of Italy, the Polish Ministry of Science and Higher Education, the Romanian Authority for Scientific Research UEFISCDI (PNII-IDEI grants 271/2011 and 17/2011), and the German-Mexican bilateral collaboration grants (DAAD-CONACYT 2009-2012, 2015-2016). J.C.A.V. acknowledges the partial support of CONACyT (grant CB-2008/106717) and the Coordinación de la Investigación Científica de la Universidad Michoacana.

References

[1] S. Ostapchenko, Proc. of the *XXV ECRS*, eConf C16-09-04.3 (2016), [astro-ph/1612.09461v1].
[2] F. Riehn et al., Proc. of the *34th ICRC*, PoS(ICRC2015)558.
[3] W.D. Apel et al., *NIM A* **620** (2010) 202.
[4] L. Cazon et al., *Astrop. Phys.* **21** (2004) 71; L. Cazon et al., *Astrop. Phys.* **23** (2005) 393.
[5] Apel W. D. et al., *NIM A* **620** (2010) 202.
[6] A.Fasso et al., Report CERN-2005-10,INFN/TC-05/11, SLAC-R-773 (2005).
[7] D. Heck et al., Report FZKA 6019, Forschungszentrum Karlsruhe (1998).
[8] R. Brun, F. Carminati, CERN Program Library Long Writeup (1993) W5013.
[9] J.C. Arteaga-Velázquez et al., Proc. of the *34th ICRC*, PoS(ICRC2015)314.
[10] S.S. Ostapchenko, *Nucl. Phys. B (Proc. Suppl.)* **151** (2006) 143; S. Ostapchenko, *Phys. Rev. D* **74** (2006) 014026.
[11] S.S. Ostapchenko, *Phys. Rev. D* **83** (2011) 014018.
[12] T. Pierog et al., Report FZKA 7516, Germany (2009) 133.
[13] E.J. Ahn et al., *Phys. Rev D* **80** (2009) 094003.
[14] J. Hersil et al., *Phys. Rev. Lett.* **6** (1961) 22; D. M. Edge et al., *J. Phys. A* **6** (1973) 1612.
[15] W.D. Apel et al., *PRD* **87** (2013) 081101.
[16] W.D. Apel et al., *PRL* **107** (2011) 171104.

PoS(ICRC2017)316